AD-A134 430 AN INVESTIGATION OF STRIP LINES AND FIN LINES WITH PERIODIC STUBS(U) ILLINOIS UNIV AT URBANA ELECTROMAGNETICS LAB T KITAZAWA ET AL. OCT 83 1/1

UNCLASSIFIED UIEM-83-13 ARO-18054.6-EL DAAG29-82-K-0084 F/G 9/5 NL

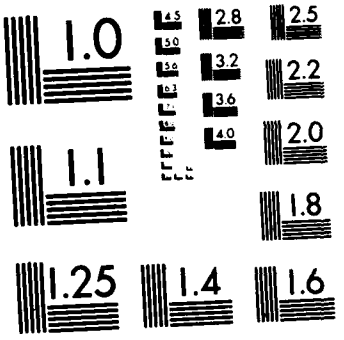

AN INVESTIGATION OF STRIP LINES AND FIN LINES WITH PERIODIC STUBS

INTERIM TECHNICAL REPORT

T. Kitazawa
R. Mittra

October 1983

SUPPORTED IN PART BY

U. S. ARMY RESEARCH OFFICE

GRANT NO. DAAG29-82-K-0084

ELECTROMAGNETICS LABORATORY
DEPARTMENT OF ELECTRICAL ENGINEERING
ENGINEERING EXPERIMENT STATION
UNIVERSITY OF ILLINOIS AT URBANA-CHAMPAIGN
URBANA, ILLINOIS 61801

UNCLASSIFIED

SECURITY CLASSIFICATION OF THIS PAGE (When Data Entered)

REPORT DOCUMENTATION PAGE		READ INSTRUCTIONS BEFORE COMPLETING FORM
1. REPORT NUMBER	2. GOVT ACCESSION NO.	3. RECIPIENT'S CATALOG NUMBER
4. TITLE (and Subtitle) AN INVESTIGATION OF STRIP LINES AND FIN LINES WITH PERIODIC STUBS		5. TYPE OF REPORT & PERIOD COVERED Interim Technical Report 6. PERFORMING ORG. REPORT NUMBER EM 83-13; UILU-ENG-83-2558
7. AUTHOR(s) T. Kitazawa and R. Mittra		8. CONTRACT OR GRANT NUMBER(s) Supported in part by DAAG29-82-K-0084
9. PERFORMING ORGANIZATION NAME AND ADDRESS Electromagnetics Laboratory Department of Electrical Engineering University of Illinois, Urbana, Illinois 61801		10. PROGRAM ELEMENT, PROJECT, TASK AREA & WORK UNIT NUMBERS P18054-EL
11. CONTROLLING OFFICE NAME AND ADDRESS U. S. Army Research Office P. O. Box 12211 Research Triangle Park, N.C. 27709		12. REPORT DATE October 1983 13. NUMBER OF PAGES 23
14. MONITORING AGENCY NAME & ADDRESS(if different from Controlling Office)		15. SECURITY CLASS. (of this report) UNCLASSIFIED 15a. DECLASSIFICATION/ DOWNGRADING SCHEDULE

16. DISTRIBUTION STATEMENT (of this Report)

Distribution Unlimited.

Approved for public release.

17. DISTRIBUTION STATEMENT (of the abstract entered in Block 20, if different from Report)

18. SUPPLEMENTARY NOTES

The findings in this report are not to be construed as an official Department of the Army position, unless so designated by other authorized documents.

19. KEY WORDS (Continue on reverse side if necessary and identify by block number)

fin-lines; strip lines; millimeter waves; periodic stub filters

20. ABSTRACT (Continue on reverse side if necessary and identify by block number)

In this paper a technique based on the network analytical formalism of electromagnetic fields is used to analyze the strip and fin lines with periodic stubs. Numerical results for the dispersion characteristics of the periodically loaded lines are presented. The effect of the loading stubs on the passband and stopband characteristics is investigated.

DD FORM 1 JAN 73 1473 EDITION OF 1 NOV 65 IS OBSOLETE

UNCLASSIFIED

SECURITY CLASSIFICATION OF THIS PAGE (When Data Entered)

UILU-ENG-83-2558

Electromagnetics Laboratory Report No. 83-13

AN INVESTIGATION OF STRIP LINES AND FIN LINES WITH PERIODIC STUBS

by

T. Kitazawa
R. Mittra

Electromagnetics Laboratory
Department of Electrical Engineering
University of Illinois at Urbana-Champaign
Urbana, Illinois 61801

Interim Technical Report

October 1983

Supported in part by

U. S. Army Research Office
Contract No. DAAG29-82-K-0084

A1

TABLE OF CONTENTS

I. INTRODUCTION

Propagation characteristics of planar transmission lines for microwave and millimeter-wave integrated circuits have been investigated in the past by many authors. Two of the frequently used transmission media in the microwave frequency range are the strip and slot lines while the fin-line is known to find applications in the millimeter-wave range. Hybrid-mode analyses of uniform lines of the above types [1] have been reported in the literature [2]. However, the periodic-loaded version of these lines finds useful applications in many devices, such as filters [3].

In this paper an approach for analyzing periodically loaded strip lines and fin lines is presented. The network-analytical method is employed for the formulation of an integral equation for the unknown electromagnetic fields [4] and Galerkin's procedure is used to derive a numerical solution of this equation. Numerical results present the passband and stopband properties.

II. THE NETWORK FORMULATION OF THE PROBLEM

In this section we illustrate the network-analytical method of formulation by analyzing the problem of fin lines with periodic stubs (see Fig. 1a), although the method itself is applicable to the strip-line configuration (Fig. 1b). The numerical results for both cases will be presented in the next section.

As a first step, we express the transverse (to z) fields in each region by using the Fourier transformation in the x-direction and Floquet harmonic representation in the y-direction as follows:

$$\left.\begin{matrix} E_t^{(i)}(x,y,z) \\ H_t^{(i)}(x,y,z) \end{matrix}\right\} = \sum_{\ell=1}^{2} \sum_{m=0}^{\infty} \sum_{n=-\infty}^{\infty} \begin{cases} V_{\ell mn}^{(i)}(z)\, e_{\ell mn}(x,y) \\ I_{\ell mn}^{(i)}(z)\, h_{\ell mn}(x,y) \end{cases} \qquad (1)$$

$$i = 1, 2, 3 \quad \text{(regions)}$$

where

$$e_{1mn}(x,y) = \sqrt{\frac{\eta_m}{2Ap}} \frac{1}{K} \{x_0 \gamma_m \cos \gamma_m(x + A) - y_0 j\beta_n \sin \gamma_m(x + A)\}\, e^{-j\beta_n y}$$

$$e_{2mn}(x,y) = \sqrt{\frac{\eta_m}{2Ap}} \frac{1}{K} \{x_0 j\beta_n \cos \gamma_m(x + A) - y_0 \gamma_m \sin \gamma_m(x + A)\}\, e^{-j\beta_n y}$$

$$h_{\ell mn}(x,y) = z_0 \times e_{\ell mn}(x,y) \qquad (\ell = 1, 2)$$

$$K^2 = \gamma_m^2 + \beta_n^2 \quad , \quad \gamma_m = \frac{m\pi}{2A} \quad , \quad \beta_n = \beta_0 + \frac{2n\pi}{p}$$

$$\eta_m = \begin{matrix} 1 & (m = 0) \\ 2 & (m \neq 0) \end{matrix} \quad \text{Neumann's number } \epsilon_m \qquad (2)$$

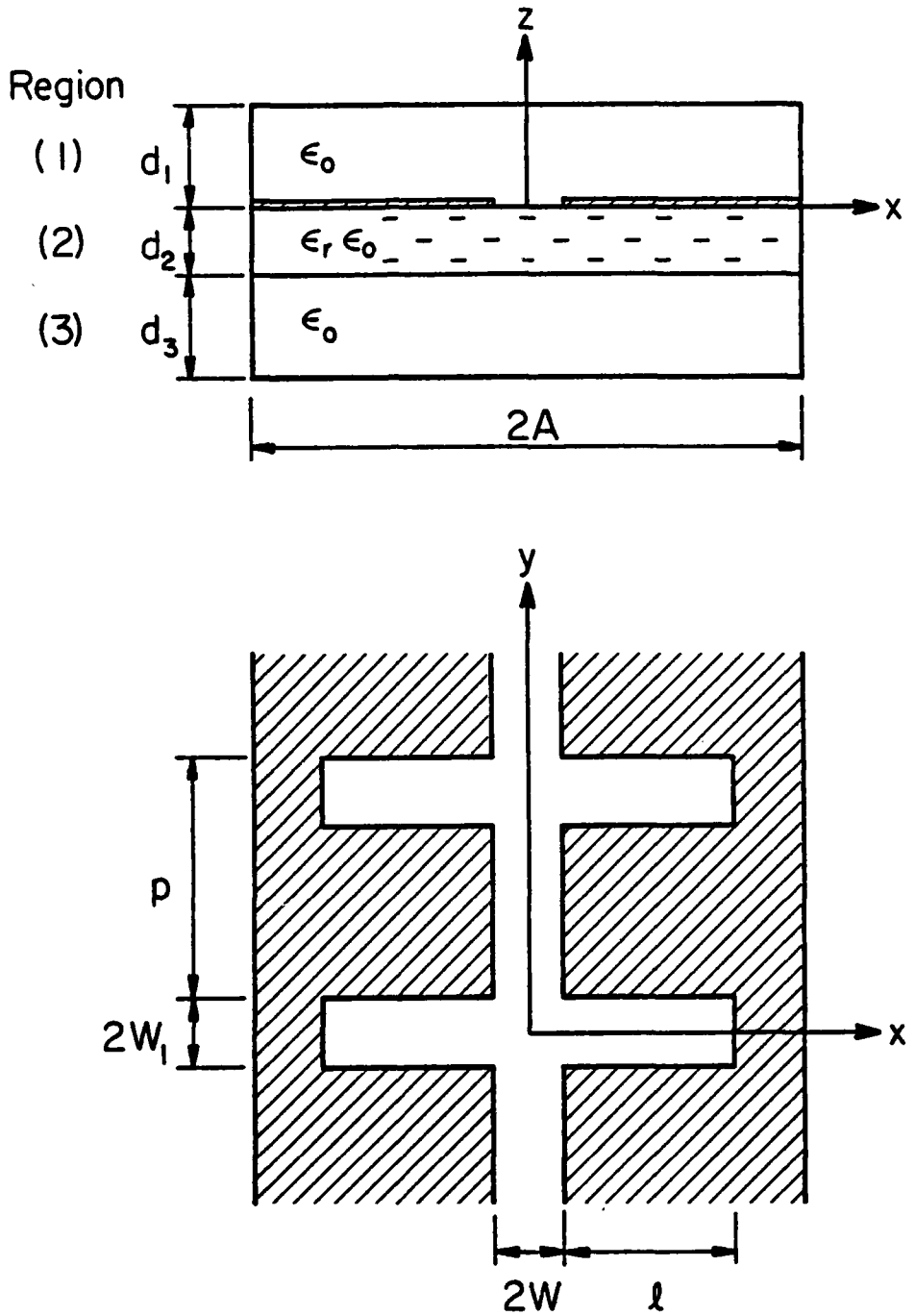

(a)

Figure 1a: Planar transmission lines with stubs - periodic-loaded fin line.

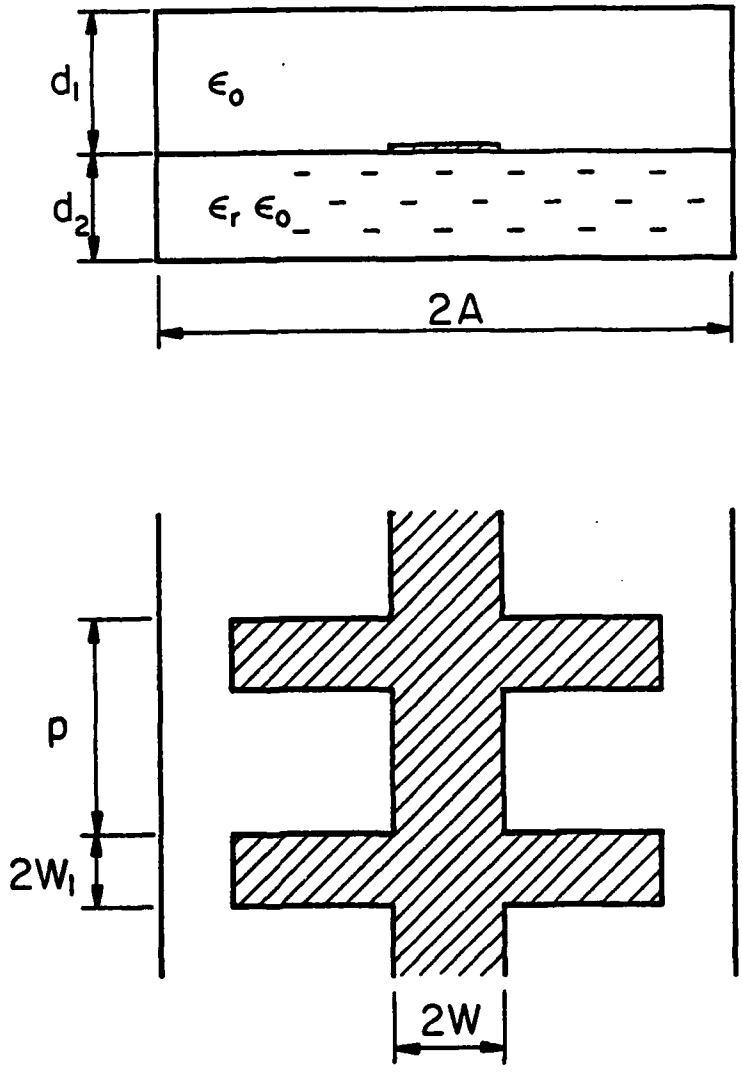

Figure 1b: Planar transmission lines with stubs - periodic-loaded strip line.

Here β_0 is the propagation constant of the dominant harmonic in the Floquet representation, and the vector mode functions $e_{\ell mn}$, $h_{\ell mn}$ satisfy the boundary conditions at $x = \pm A$ as well as the following orthonormal properties:

$$\int_{-A}^{A} \int_{-P/2}^{P/2} e_{\ell mn}(x,y) \cdot e^{*}_{\ell' m' n'}(x,y)\, dxdy = \delta_{\ell\ell'}\ \delta_{mm'}\ \delta_{nn'} \tag{3}$$

where $\delta_{\ell\ell'}$ is Kronecker's delta and the symbol * signifies complex conjugate. Substituting (1) into Maxwell's field equations and applying the orthonormal properties (3), we obtain the differential equations for $V^{(i)}_{\ell mn}$ and $I^{(i)}_{\ell mn}$:

$$\begin{cases} -\dfrac{dV^{(i)}_{\ell mn}}{dz} = j\kappa^{(i)}_{mn}\ z^{(i)}_{\ell mn}\ I^{(i)}_{\ell mn} \\ \\ -\dfrac{dI^{(i)}_{\ell mn}}{dz} = j\kappa^{(i)}_{mn}\ y^{(i)}_{\ell mn}\ V^{(i)}_{\ell mn} \end{cases} \tag{4}$$

where

$$z^{(i)}_{1mn} = \frac{\kappa^{(i)}_{mn}}{\omega\epsilon_0\epsilon_r^{(i)}}\ , \qquad z^{(i)}_{2mn} = \frac{\omega\mu_0}{\kappa^{(i)}_{mn}}$$

$$y^{(i)}_{\ell mn} = \frac{1}{z^{(i)}_{\ell mn}}\ , \qquad \kappa^{(i)}_{mn} = \sqrt{k^2\ \epsilon_r^{(i)} - K^2}\ ,$$

$$k = \omega\sqrt{\epsilon_0\mu_0}\ , \qquad \epsilon_r^{(i)} = \begin{cases} \epsilon_r & \text{(region (2))} \\ 1 & \text{(otherwise)} \end{cases}\ . \tag{5}$$

The boundary conditions to be satisfied are expressed as follows:

$$V_{\ell mn}^{(1)}(d_1) = 0 \tag{6}$$

$$V_{\ell mn}^{(1)}(+0) = V_{\ell mn}^{(2)}(-0) = v_{\ell mn} \tag{7}$$

$$V_{\ell mn}^{(2)}(-d_2 + 0) = V_{\ell mn}^{(3)}(-d_2 - 0) \tag{8a}$$

$$I_{\ell mn}^{(2)}(-d_2 + 0) = I_{\ell mn}^{(3)}(-d_2 - 0) \tag{8b}$$

$$V_{\ell mn}^{(3)}(-d_2 - d_3) = 0 \tag{9}$$

and

$$H_t^{(i)}(x,y,+0) = H_t^{(2)}(x,y,-0) \tag{10}$$

(in the aperture of $z = 0$)

where

$$v_{\ell mn} = \int_{-A}^{A} \int_{-P/2}^{P/2} e^{*}_{\ell mn}(x',y') \cdot \varepsilon(x',y')\, dx'dy' \tag{11}$$

and $\varepsilon(x,y)$ is the transverse electric field in the aperture at $z = 0$.

Solution of the differential equations (4) and imposition of the boundary conditions (6) - (9) yield the unknowns $V_{\ell mn}^{(i)}$ and $I_{\ell mn}^{(i)}$ in each region. The electromagnetic fields, in turn, can be obtained by substituting $V_{\ell mn}^{(i)}$ and $I_{\ell mn}^{(i)}$ into Equation (1). Finally, applying the remaining boundary conditions (10), we may obtain the integral equation for the aperture field $\varepsilon(x,y)$, and implicitly for the unknown propagation constant β_0:

$$\sum_m \sum_n \int_{-A}^{A} \int_{-P/2}^{P/2} \{Y_{1mn}\, h_{1mn}(x,y)\, e^{*}_{1mn}(x',y') + Y_{2mn}\, h_{2mn}(x,y)\, e^{*}_{2mn}(x',y')\}$$

$$\cdot \varepsilon(x',y')\, dx'dy' = 0 \tag{12}$$

where (x,y) lies in the aperture at z = 0 and

$$Y_{1mn} = \omega\varepsilon_0 \left\{ \frac{1}{\kappa_{mn}^{(1)}} \cot\left(\kappa_{mn}^{(1)} d_1\right) + \frac{\varepsilon_r}{\kappa_{mn}^{(2)}} \frac{\kappa_{mn}^{(2)} - \varepsilon_r \kappa_{mn}^{(3)} \tan\left(\kappa_{mn}^{(2)} d_2\right) \tan\left(\kappa_{mn}^{(3)} d_3\right)}{\kappa_{mn}^{(2)} \tan\left(\kappa_{mn}^{(2)} d_2\right) + \varepsilon_r \kappa_{mn}^{(3)} \tan\left(\kappa_{mn}^{(3)} d_3\right)} \right\}$$

$$Y_{2mn} = \frac{1}{\omega\mu_0} \left\{ \kappa_{mn}^{(1)} \cot\left(\kappa_{mn}^{(1)} d_1\right) + \kappa_{mn}^{(2)} \frac{\frac{1}{\kappa_{mn}^{(2)}} - \frac{1}{\kappa_{mn}^{(3)}} \tan\left(\kappa_{mn}^{(2)} d_2\right) \tan\left(\kappa_{mn}^{(3)} d_3\right)}{\frac{1}{\kappa_{mn}^{(2)}} \tan\left(\kappa^{(2)} d_2\right) + \frac{1}{\kappa_{mn}^{(3)}} \tan\left(\kappa_{mn}^{(3)} d_3\right)} \right\} . \quad (13)$$

The formulation is rigorous up to this stage. The numerical computation for the above equation is explained in the next section.

III. NUMERICAL COMPUTATION AND RESULTS

Equation (12) can be expressed in an operator form as

$$\bar{\bar{F}}(x,y|x',y')\cdot\varepsilon(x',y') = 0 \tag{14}$$

where the dyadic operator $\bar{\bar{F}}\cdot$ is given by

$$\bar{\bar{F}}(x,y|x',y')\cdot = \sum_m \sum_n \int_{-A}^{A} \int_{-P/2}^{P/2} \{Y_{1mn}\, h_{1mn}(x,y)\, e^*_{1mn}(x',y')$$

$$+ Y_{2mn}\, h_{2mn}(x,y)\, e^*_{2mn}(x',y')\}\, dx'dy'\cdot \tag{15}$$

The determinantal equation for the dispersion relation can be obtained by applying Galerkin's procedure to Eq. (14). In this procedure, the unknown aperture field $\varepsilon(x,y)$ is expanded in terms of the appropriate basis functions $f_k(x,y)$ as follows:

$$\varepsilon(x,y) = \sum_{k=1}^{N} a_k\, f_k(x,y) \tag{16}$$

where a_k are the unknown coefficients. Substituting (16) into (14), using $f^*_m(x,y)$ as test functions and taking inner products, we obtain a set of simultaneous equations for the unknown coefficients a_k:

$$[M]\,[a] = 0\ . \tag{17a}$$

That is,

$$\begin{bmatrix} M_{11} & M_{12} & \cdots & M_{1N} \\ M_{21} & \cdot & & \\ \cdot & & \cdot & \\ \cdot & & & \cdot \\ M_{N1} & & & M_{NN} \end{bmatrix} \begin{bmatrix} a_1 \\ a_2 \\ \cdot \\ \cdot \\ a_N \end{bmatrix} = 0 \tag{17b}$$

where

$$M_{mk} = \int_{-A}^{A} \int_{-P/2}^{P/2} Z_0 \times f_m^*(x,y) \cdot \{\bar{\bar{F}}(x,y|x',y') \cdot f_k(x',y')\}\, dxdy \ . \tag{18}$$

The determinantal equation for the propagation constant β_0 can be obtained by setting the determinant of the coefficient matrix of Eq. (17) equal to zero, i.e.,

$$\det[M(\beta_0)] = 0 \ . \tag{19}$$

It remains only to select the basis functions $f_k(x,y)$. Before defining the basis functions, we introduce three auxiliary functions:

$$S_1(x,y) = \begin{cases} 1 & \left(|x| \le W \text{ and } |y| \le \frac{P}{2}\right) \\ 0 & \text{(otherwise)} \end{cases}$$

$$S_2(x,y) = \begin{cases} 1 & \left(|x| \le W \text{ and } W_1 \le |y| \le \frac{P}{2}\right) \\ 0 & \text{(otherwise)} \end{cases}$$

$$S_3(x,y) = \begin{cases} 1 & \left(W \le |x| \le W + \ell \text{ and } |y| \le W_1\right) \\ 0 & \text{(otherwise)} \end{cases} \tag{20}$$

The regions represented by these functions are shown in Fig. 2. The basis functions to be used are defined by employing these auxiliary functions:

$$f_1(x,y) = x_0\, X(x)\, e^{-j\beta_0 y}\, S_1(x,y) \tag{21a}$$

$$f_2(x,y) = x_0\, X(x)\, e^{-j\beta_{-1} y}\, S_1(x,y) \tag{21b}$$

$$f_3(x,y) = x_0\, \mathrm{sgn}(y)\, X(x)\, e^{-j\beta_0 y}\, S_2(x,y) + y_0\, \mathrm{sgn}(x) \cos\left\{\frac{\pi}{2(\ell + W)} x\right\} Y(y)\, S_3(x,y) \tag{21c}$$

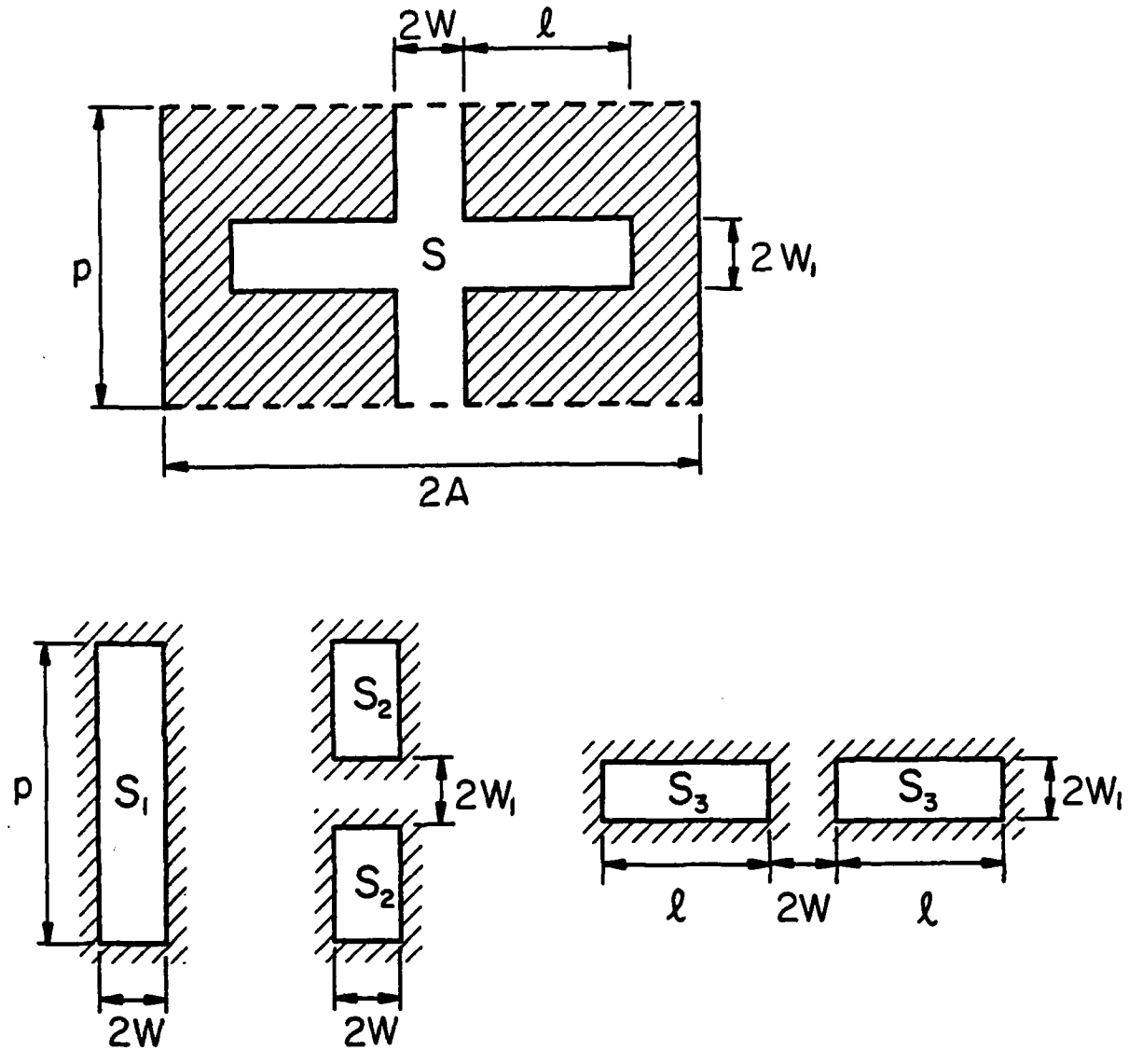

Figure 2: Regions represented by Equation (20).

$$f_4(x,y) = x_0 \, \mathrm{sgn}(y) \, X(x) \, e^{-j\beta_{-1}y} \, S_2(x,y)$$

$$+ y_0 \, \mathrm{sgn}(x) \cos\left\{\frac{\pi}{2(\ell + W)} x\right\} Y(y) \, S_3(x,y) \qquad (21d)$$

where

$$\beta_{-1} = \beta_0 - \frac{2\pi}{p}$$

and X(x) and Y(y) represent the x- and y-variations in the main- and stub-fin lines, respectively. Three different functions are used for X(x) and Y(y), viz.,

$$\text{i)} \quad X(x) = \frac{C}{W} \;, \quad Y(y) = \frac{C}{W_1} \qquad C: \text{ constant}$$

$$\text{ii)} \quad X(x) = \frac{|x|}{W} \;, \quad Y(y) = \frac{|y|}{W_1}$$

$$\text{iii)} \quad X(x) = \frac{1}{W}\left\{1 + \left|\frac{x}{W}\right|^3\right\} \;, \quad Y(y) = \frac{1}{W_1}\left\{1 + \left|\frac{y}{W_1}\right|^3\right\} \;. \qquad (22)$$

We mention that the functions in (21c) and (21d) are quite similar in character to the junction basis functions that have been employed in scattering problems [5].

Figure 3 shows the $k - \beta_0$ diagram for a fin line with periodic stubs. Computations have been performed for three different sets of basis functions given in (22), but the deviations were found to be rather small because Galerkin's procedure was used in the numerical computations. The curve for the periodically loaded fin line (solid line) is lower than for the uniform fin line without stubs (broken line) because of the inductive reactance of the series stubs. The passband and stopband regions, which are common in the dispersion diagrams in periodic structures [6] and are applicable to filters, are clearly

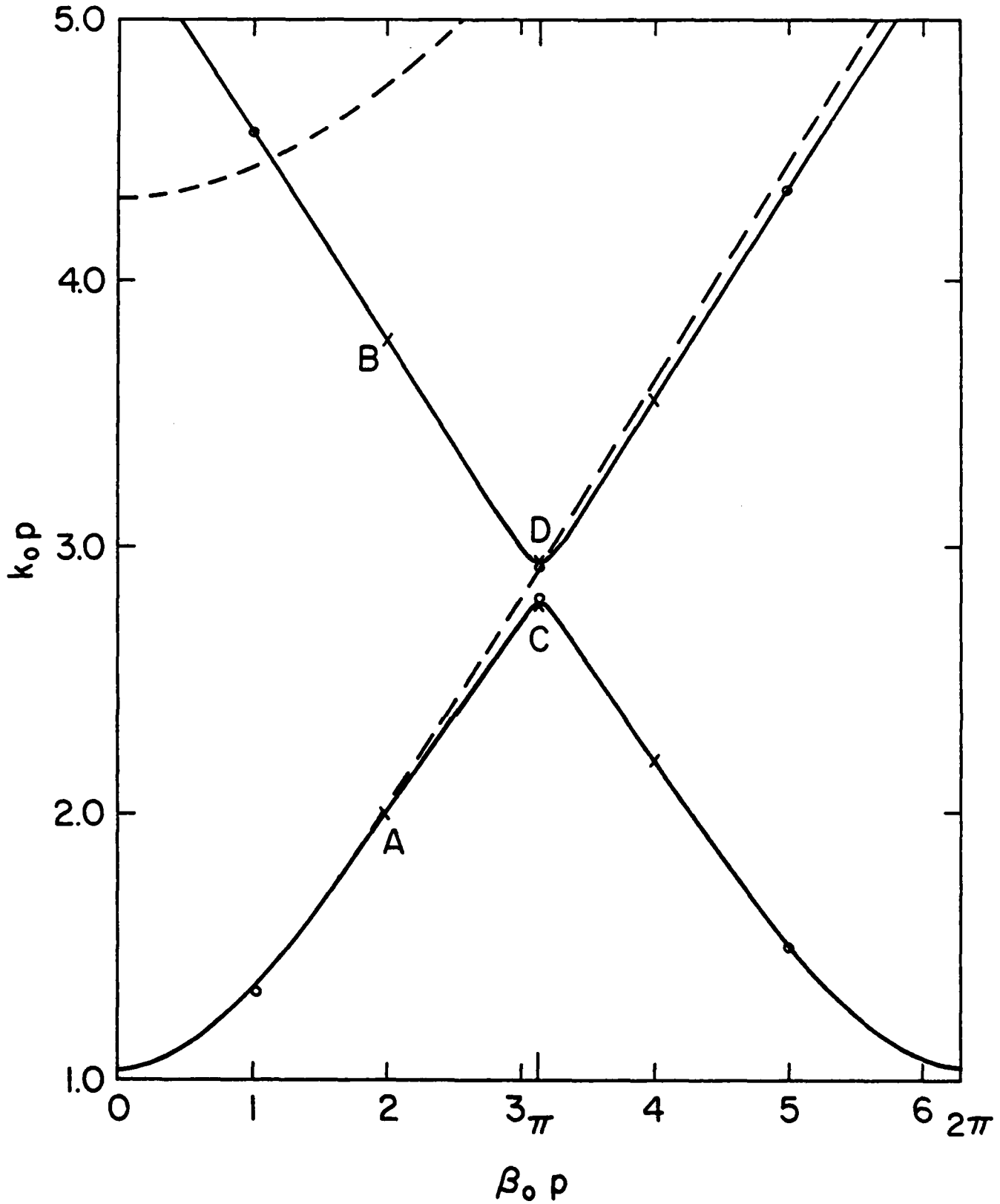

Figure 3: The k - β_0 diagram for a periodic-loaded fin line. ε_r = 2.2, d_1 = 0.094", d_2 = 0.005", d_3 = 0.089", W = 0.0025", A = 0.047", W_1 = 0.01", ℓ = 0.04", p = 0.12" ———: fin line with stubs using iii) in (22), ------: uniform fin line (without stubs), 0: using i) in (22), X: using ii) in (22).

evident in Fig. 3. The first passband occurs in the frequency range when kp satisfies $1.038 < kp < 2.800$ and the first stopband $2.800 < kp < 2.931$. It should be noted that the higher-order stopbands will appear in the higher-frequency range; however, since the higher-order (even) mode of the uniform fin line (without stubs) can propagate in the range $kp > 4.315$, these higher stopbands have little significance.

Figure 4 shows the relative amplitude of the coefficients of basis functions f_1 and f_2, which represent the $n = 0$ and $n = -1$ harmonics, respectively, at each point indicated in Fig. 3. These results show that the first stopband is caused by the coupling between the $n = 0$ and $n = -1$ harmonics.

Figure 5 shows the effect of the loading stubs on the normalized stopband width $\Delta k/k_c$, where Δk is the stopband width and k_c is the center frequency. The stub length ℓ is smaller than the quarter wavelength of the stub fin line, so the series stubs have an inductive reactance; therefore, the longer the stub, the wider the stopband. The characteristic impedance of the fin line becomes larger as the gap becomes wider [2]; therefore, the stopband becomes wider with wider stubs, although the dependence on the stub width is relatively small.

Figure 6 shows the $k - \beta_0$ diagram of the strip line with periodic stubs. Again, the passband and stopband properties are observed in this case, with the first passband occurring when $0 < kp < 1.228$ and the first stopband when $1.228 < kp < 1.286$. The first higher-order mode of the main strip line appears when $kp = 2.289$; therefore, the higher-order stopbands have no meaning in the same way as the case of fin line.

Figure 7 shows the effect of the loading stubs. The characteristic impedance of the strip line becomes smaller as the strip becomes wider [4], but the stubs are shunt-connected in this case. Therefore, the stopband, again, becomes wider with wider stubs.

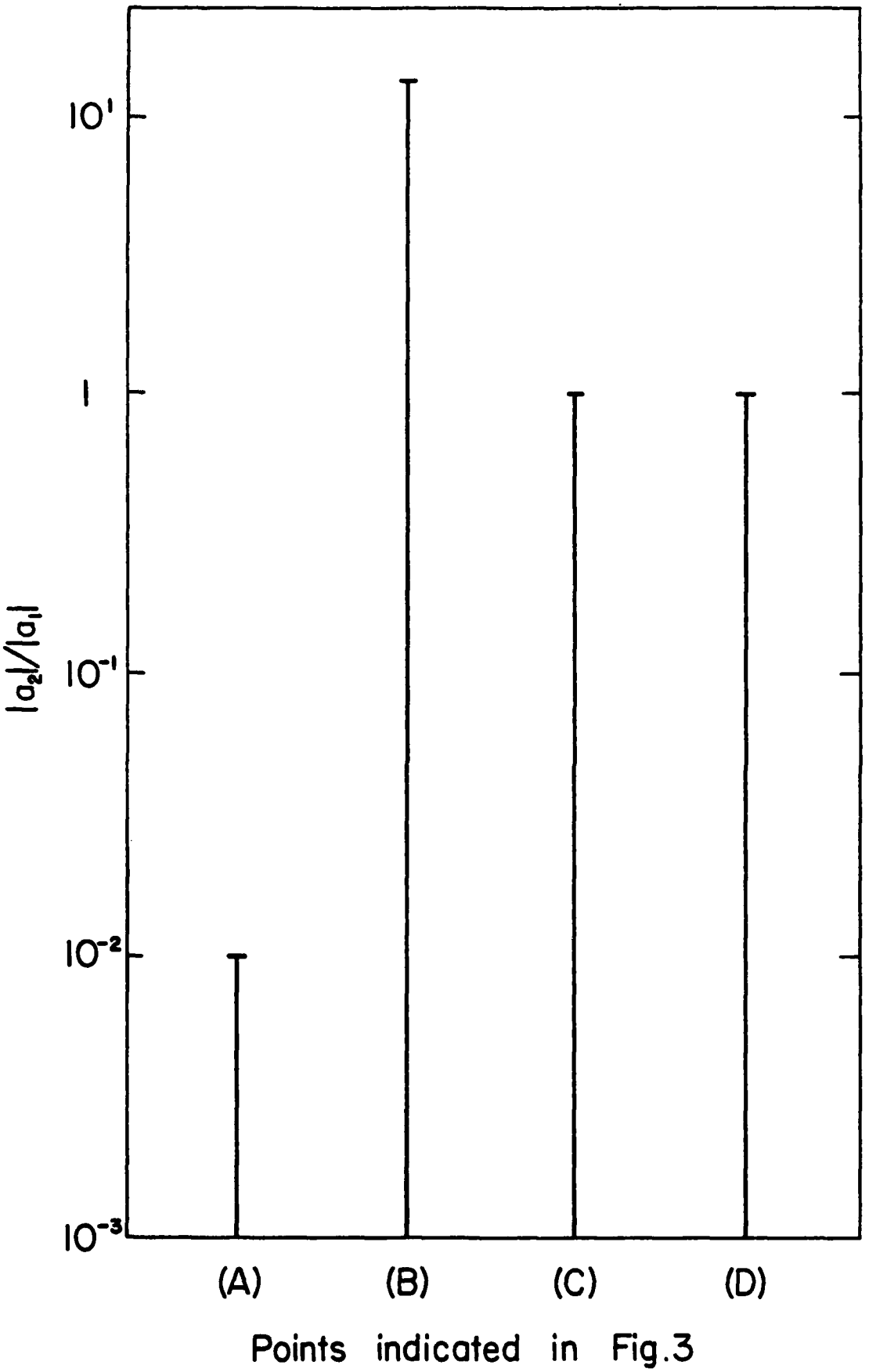

Figure 4: The relative amplitude of coefficients of basis functions f_1 and f_2.

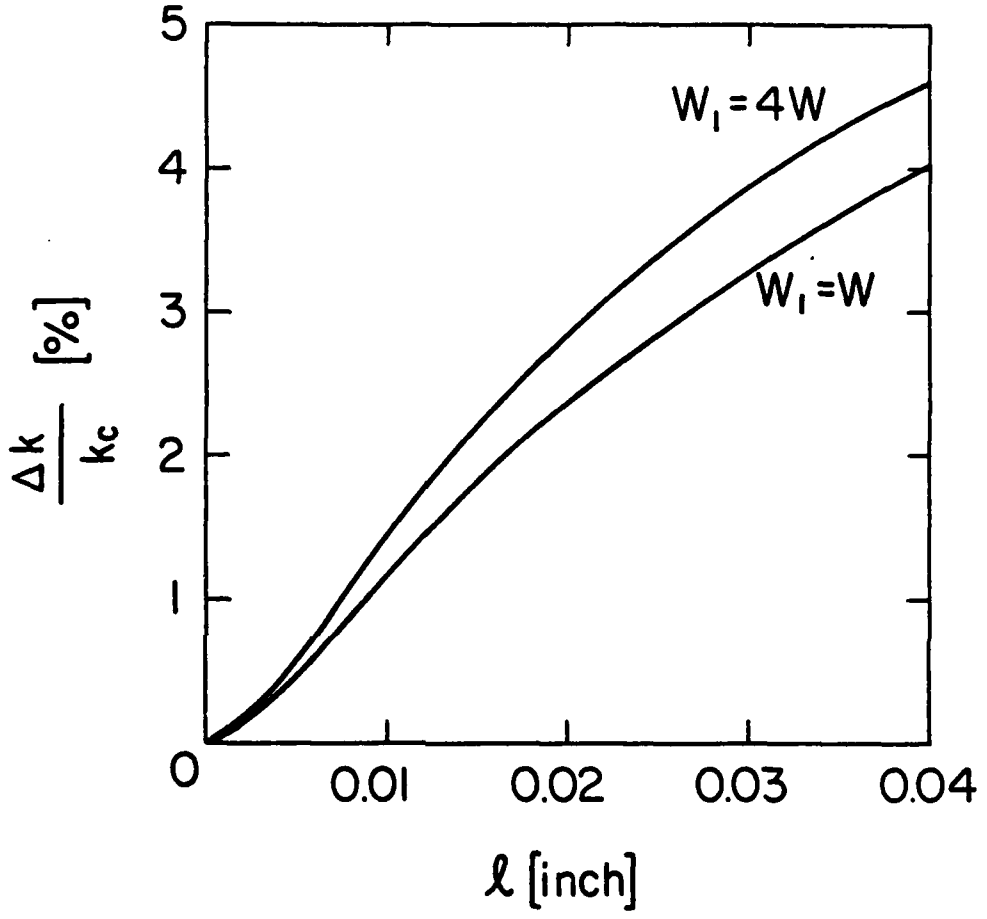

Figure 5: The effect of the loading stubs of the fin line. $\varepsilon_r = 2.2$, $d_1 = 0.094"$, $d_2 = 0.005"$, $d_3 = 0.089"$, $W = 0.0025"$, $A = 0.047"$, $p = 0.12"$.

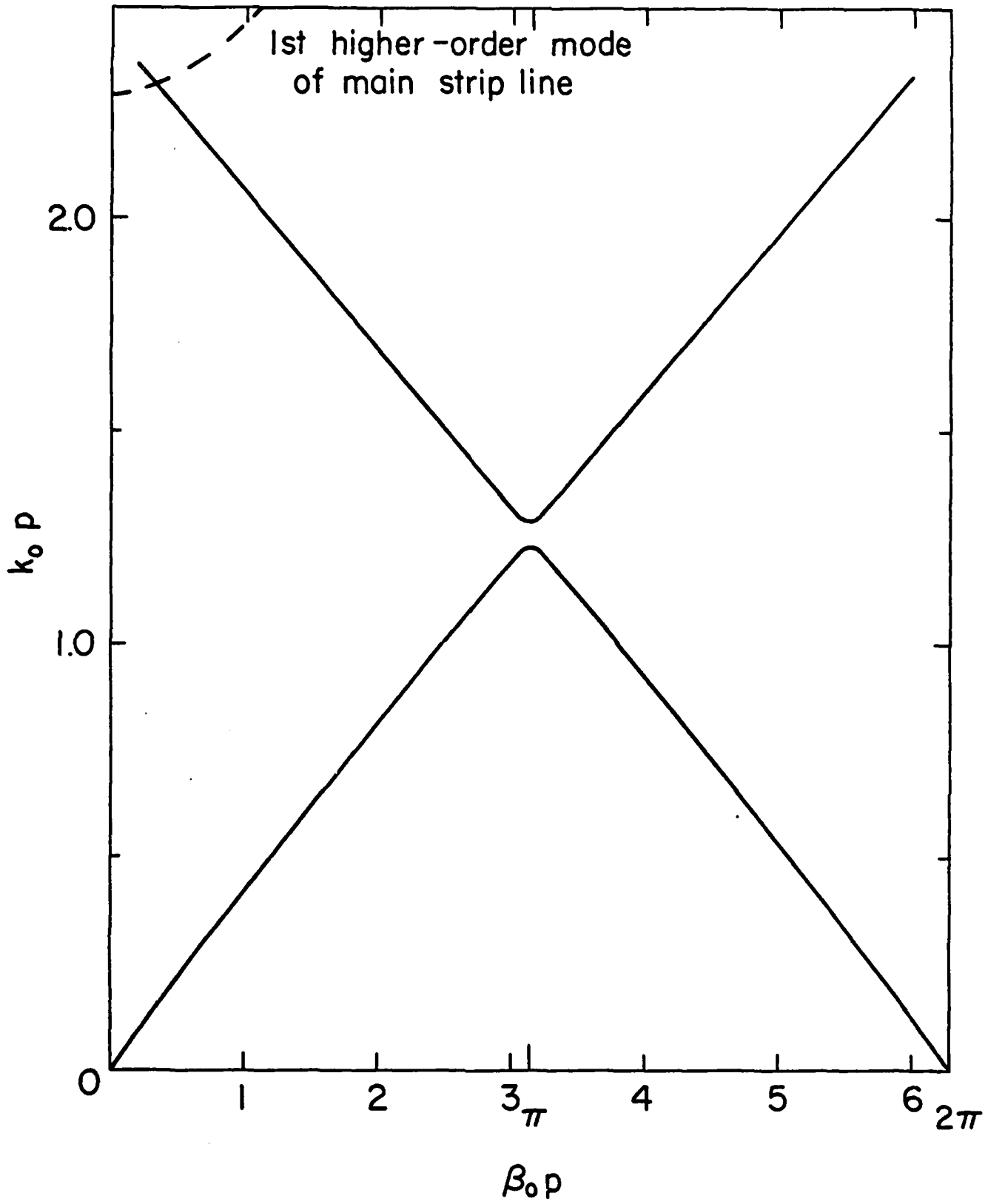

Figure 6: The k - β_0 diagram for a periodic-loaded strip line.
ε_r = 8.875, d_1 = 11.43(mm), d_2 = 1.27(mm), W = 0.3175(mm),
A = 6.35(mm), W_1 = 0.3175(mm), 1 = 4(mm), p = 10(mm).

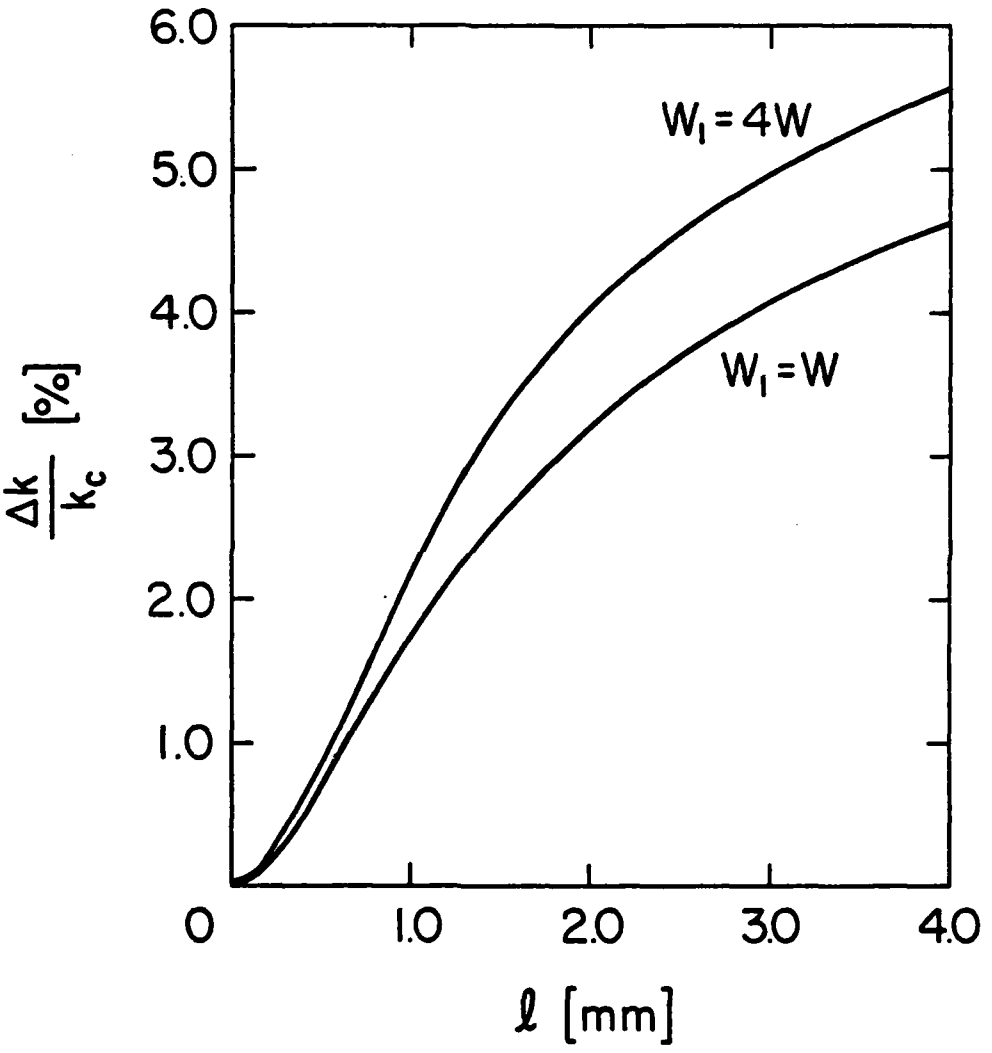

Figure 7: The effect of the loading stubs of the strip line.
$\varepsilon_r = 8.875$, $d_1 = 11.43$(mm), $d_2 = 1.27$(mm), $W = 0.3175$(mm),
$A = 6.35$(mm), $p = 10$(mm).

IV. CONCLUSIONS

A method of analysis for the strip line and the fin line with periodic stubs has been presented, and the $k - \beta_0$ diagrams for these structures have been computed. It is found that the passband and stopband properties are generated from the coupling between the $n = 0$ and $n = -1$ harmonics. The effects of the loading stubs have been determined numerically.

REFERENCES

[1] G. Kowalski and R. Pregla, "Dispersion characteristics of shielded microstrips with finite thickness," Arch. Elek. Ubertragung, vol. 25, pp. 193-196, April 1971.

[2] Y. Hayashi, E. Farr, S. Wilson, and R. Mittra, "Analysis of dominant and higher-order modes in unilateral fin lines," Arch. Elek, Ubertragung, vol. 37, pp. 117-122, March 1983.

[3] H. Entschladen and H. J. Siweris, "Slot line stub filters," Arch. Elek. Ubertragung, vol. 34, pp. 152-156, April 1980.

[4] T. Kitazawa and Y. Hayashi, "Propagation characteristics of strip lines with multilayered anisotropic media," IEEE Trans. Microwave Theory Tech., to be published.

[5] C. H. Tsao and R. Mittra, "Spectral-domain analysis of frequency selective surfaces (FSS) comprised of periodic arrays of cross-dipoles and Jerusalem-crosses," to appear in IEEE Trans. Antennas Propagat.

[6] R. E. Collin, Field Theory of Guided Waves. New York: McGraw-Hill, 1960, p. 368.